MolecularLibraries
Pathways to Discovery

Probe Report

Title: ML345, A Small-Molecule Inhibitor of the Insulin-Degrading Enzyme (IDE)

Authors: Bannister TD[1], Wang H[1], Abdul-Hay SO[2], Masson A[2], Madoux F[3], Ferguson J[3], Mercer BA[3], Schurer S[4], Zuhl A[5], Cravatt BF[5], Leissring MA[2], Hodder P[3]*

[1]Scripps Research Institute Department of Chemistry, Translational Research Institute, Jupiter, Florida 33458**;** [2]Department of Neuroscience, Mayo Clinic, Jacksonville, FL 32224; **[3]**Scripps Research Institute Molecular Screening Center, Lead Identification Division, Translational Research Institute, Jupiter, Florida 33458; [4]University of Miami, Miller School of Medicine, Miami FL 33136. [5] Department of Chemical Physiology, TSRI, La Jolla, CA 92037; Corresponding author: hodderp@scripps.edu

Abstract: Insulin-degrading enzyme (IDE) is a thiol-sensitive zinc-metallopeptidase that is strongly implicated in the pathogenesis of multiple highly prevalent diseases, including type 2 diabetes and Alzheimer's disease (AD). Because IDE is *the* principal insulin-degrading protease *in vivo,* IDE inhibitors should enhance insulin signaling and thus have efficacy in relevant animal models of diabetes and also in therapy. Despite decades of study, a strong need yet exists for the identification of potent, selective, *in vivo* stable small molecule experimental probes that inhibit IDE with significantly high potency and target selectivity. We herein describe an IDE inhibitor molecular probe, ML345, which targets a specific cysteine residue (Cys819) in IDE. ML345 arose from an ultra high-throughput screening (uHTS) campaign that was supplemented with medicinal chemistry SAR optimization and with biochemical mechanistic profiling efforts. The probe is distinguished from prior art inhibitors, such as the potent and selective (but peptide-derived) hydroxamic acids and from weaker and far less selective small molecules that have been described in the literature. Probe ML345 is well-suited for use as a pharmacophore for drug development in diabetes research and as an experimental probe to understand the array of effects displayed by IDE in biological systems.

Probe Structure & Characteristics:
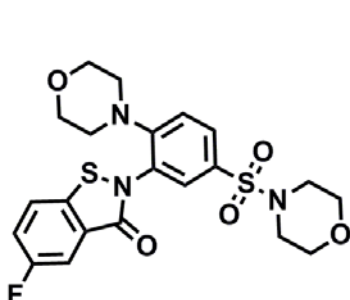
ML345
CID57390068
SID144241486
SR-03000002959-2
MW 479.5
cLogP 2.0
tPSA 113
H-bond donors: 0
H-bond acceptors: 7
Ro5 compliant

CID/ML#	Target Name	EC_{50} [SID, AID]	Anti-target(s)	IC_{50} [SID, AID]	Fold Selective	Secondary Assay(s): IC_{50} (nM) [SID, AID]
CID 57390068 SID 136920229 synthesized (small scale) SID 144241486 synthesized (larger scale) **ML345**	IDE	IC_{50} = 188 nM [SID 136920229, AID 624065]	HEK cytotoxicity	EC_{50} >10 μM (inactive) [SID136920229, AID 588709]	>50	IC_{50} >100 μM, cysteine null mutant IDE enzyme [SID 136920229, AID 624338] Activity-based protein profiling analysis: minimal effects vs. the cysteine-reactive proteome @ 2 μM [SID 144241486, AID pending]

Batch data, IDE Inhibitor Probe

CID	SID	source	Purity
57390068	136920229	Scripps synthesis	>98%, (HPLC, MS, NMR)
57390068	144241486	Scripps synthesis	>98% (HPLC, MS, NMR)
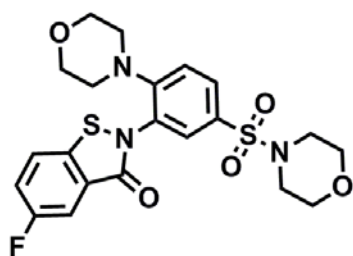
Probe ML345 chemical descriptors and highlighted properties

Physical Properties (measured at the SRIMSC):

Stability ($t_{1/2}$) in PBS: >>48 hours
$t_{1/2}$, liver microsome stability:
>120 min (human), 24 min (mouse), 50 min (rat)
CYP450 inhib. 81%, 75%, 57%, 90%
@10 μM (1A2, 2D6, 3A4, 2C9)
Solubility in PBS = 0.4 μM
Solubility in simulated general assay buffer = 5.1 μM

Other attributes of ML345:
The probe is readily synthesized,
rule-of-five compliant,
target-selective (as determined by activity-based protein profiling),
has a defined mechanism of action,
has IDE activity that greatly exceeds the small molecule prior art.

Recommendations for scientific use of the probe: The IDE inhibitor probe ML345 will be used to understand how IDE processes its natural substrates, including insulin and beta-amyloid, defining the effects of disrupting IDE's actions. The probe and derived follow-up compounds may show efficacy in models of insulin homeostasis, both in cell culture and in animal models. It is anticipated that IDE inhibitors can enhance insulin signaling, perhaps in synergy with agents such as GLP-1 agonists and DPPIV inhibitors, thus providing an opportunity for a significant advance in anti-diabetes therapy.

1   Introduction

Overview. Insulin-degrading enzyme (IDE) is a thiol-sensitive zinc-metallopeptidase that is strongly implicated in the pathogenesis of multiple highly prevalent diseases, including type 2 diabetes[1,2], Alzheimer's disease (AD)[2,3], and Varicella-Zoster virus (VZV) infection[4]. IDE is the primary protease responsible for insulin degradation *in vivo*[1,2], mediating the critical, final step of insulin action, the termination of the insulin response[5]. IDE inhibitors thus should enhance insulin signaling and find use in treating diabetes[5]. They may also aid wound healing[6], among other medicinal benefits.

The IDE superfamily of zinc-metalloproteases evolved separately from the widely-studied "conventional" zinc-metalloproteases, a fascinating example of convergent evolution[7]. Members of this superfamily (clan M16) are often referred to as "inverzincins" because they feature a characteristic *inverted* zinc-binding motif (HxxEH) relative to that found within most conventional zinc-metalloproteases (HExxH)[8]. This structural change alters function and may further explain why conventional zinc-metalloproteases have been targeted for small molecule inhibition often and frequently with success, while no drug-like inhibitors of IDE (or any other inverzincin family member, for that matter) are known.

IDE was discovered in 1949 by I. Arthur Mirsky, who recognized that blocking IDE-mediated insulin catabolism was desirable for promoting endogenous insulin signaling and, thereby, was a promising target for the treatment of type 2 diabetes[9]. Mirsky showed that a purified, non-proteinaceous endogenous (but unknown) inhibitor of IDE could potentiate the hypoglycemic action of insulin in rabbits[10]. These and other results prompted strong interest in the development of orally bioavailable inhibitors of IDE. Indeed, several antidiabetic drugs emerged in the late 1950s that were initially *believed* to act by selective inhibition of IDE, though they were later found to act by other mechanisms[11-14]. *Truly specific and drug-like IDE inhibitors have remained elusive.*

IDE is subject to inhibition by chelation of the key active site zinc atom, though an inherent concern of this approach is the difficult task of achieving selectivity for IDE over the wide array of other zinc-dependent metalloproteases. Another concern is that animal toxicity is often associated with the incorporation of potent zinc-binding motifs, such as hydroxamic acids.

The Leissring group (the assay provider for this effort) has shown that IDE's actions are dependent upon two specific cysteine residues, C812 and C819[15], suggesting that thiol-modifying agents may also be IDE inhibitors. Such an approach raises the concern, however, about the potentially difficult task of attaining selectivity for IDE over the many other enzymes bearing reactive cysteine residues. IDE inhibitors that bind to allosteric sites of IDE may, in principle, also be used, though no allosteric inhibition sites of IDE have yet been identified.

IDE's unique clamshell-like macromolecular structure[15,16] and its sensitivity both to zinc chelation and to thiol modification may help explain many of its unusual structural dynamics, extraordinary pharmacological properties, and the failure of previous efforts to find small molecule modulators of its activity. The Leissring group has aimed to study and to exploit these critical features for therapeutic means, pursuing the development of IDE inhibitors (and also activators) for more than a decade[5,17-19]. Using a rational design approach, the Leissring group succeeded in developing the first potent (K_i =1.7 nM) and selective (10,000-fold selectivity vs. other zinc-metalloproteases) IDE inhibitor, a peptide-derived hydroxamic acid known as "Ii1" (IDE inhibitor 1)[5]. Despite its merits, Ii1 is not ideal as a chemical probe, especially for *in vivo* studies, owing to its high molecular weight (~750 Daltons) and its peptidic nature that renders it susceptible to rapid metabolism ($t_{1/2}$ ~9 minutes in mice).

Relevance to Type 2 Diabetes. A natural substrate for IDE, insulin, possesses a distinctive tertiary structure, with two peptide chains linked by intra- and inter-chain disulfide bonds. Insulin is quite inert to processing by most common multifunctional proteases. IDE, however, efficiently degrades insulin and other peptide substrates such as glucagon, TGF alpha, and β-endorphin[8]. IDE knockout (IDE-KO) mice confirm the *in vivo* relevance of IDE in insulin catabolism, exhibiting fasting serum insulin levels ~3-fold higher than wild-type (WT) littermates[1,2]. Moreover, insulin degradation in IDE-KO tissue extracts was shown to be decreased by as much as 97%[2]. *Because IDE is essentially the only protease that efficiently degrades insulin, inhibition of IDE is a straightforward way to augment insulin's actions experimentally and, potentially, therapeutically.*

There is also convincing evidence that IDE can regulate insulin action *via* degradation occurring downstream of insulin receptor (IR) binding[20]. For example, the Leissring group recently showed that that the activity of insulin pre-bound to its receptor is potentiated in the presence of IDE inhibitors[5], and Roth and colleagues found that the converse is true in cells over-expressing IDE[21]. These and other results strongly suggest that IDE acts to regulate the termination of insulin action within cells, likely by modulating the off rate of insulin from its receptor[5]. Effective IDE inhibitors that are sufficiently stable for long-term use in cultured cells and *in vivo* will constitute essential tools for clarifying how—and where—IDE regulates the termination of insulin action.

Besides the expected elevated fasting serum insulin levels and accelerated glucose clearance of IDE-KO mice, these animals also show pronounced *compensatory changes* that are perhaps *not* linked to effects that would be expected from pharmacological IDE inhibition, such as chronic hyperinsulinemia[1,2]. The complete systemic ablation of IDE in the knockout state, levels far lower than what might ideally be achieved pharmacologically, may lead to hyperinsulinemia and to other compensatory effects such as pronounced glucose and insulin intolerance[1]. Such effects complicate the elucidation of IDE's normal role in insulin signaling and in the pathogenesis of diabetes (as well as in other disease pathologies). Without potent and selective small molecule modulators of IDE activity available, it has been difficult to determine if such effects are artifacts that are not entirely relevant to possible IDE inhibitor therapy. We propose that such effects need *not* arise *via* short-term pharmacological inhibition of IDE, using compounds having a rapid onset of action, in adult individuals, with an ability to inhibit IDE partially and/or transiently. IDE inhibitors may also affect different pools of IDE (*e.g.;* intracellular vs. extracellular). Suitable tool compounds to cleanly assess the physiological and

pathophysiological role of IDE proteolytic activity *in vivo* are needed. Importantly, as we will show, suitable molecular probes to answer these important questions have arisen from our probe development effort.

Other roles of IDE. A recent study[4] identified IDE as the cellular receptor for Varicella-Zoster virus (VZV) infection and invasion. Recent analysis suggests that infectivity is linked to IDE activity[15], thus IDE inhibitors might be useful against VZV infection.

IDE also plays an important role in Alzheimer's disease (AD) pathogenesis, as the principal extracellular protease responsible for the degradation of Aß, an amyloidogenic peptide that accumulates in the brains of AD patients[22]. IDE-KO mice show a ~95% reduction in the rate of degradation of physiological levels of Aß applied exogenously[2]. IDE-KO mice also harbor significant increases in steady-state levels of endogenous cerebral Aß[2]. Using a transgenic approach, the Leissring group showed that a doubling of IDE levels expressed in neurons dramatically reduced steady-state brain Aß levels, amyloid plaque burden, and downstream cytopathology in a mouse model of AD[3]. Literature evidence strongly supports a link between IDE genetic variation and the incidence / onset of AD in man[23].

Because of expected Aß effects, IDE inhibitors used in diabetes therapy should not be highly brain-exposed. IDE inhibitors administered to affected brain tissue in animal models may, however, manipulate IDE activity and permit *a* more clearly assessment of its role in AD progression. Evidence of IDE inhibitory effects would support efforts to thwart the progression of AD by the use of IDE *activators*, which are the subject of another ongoing MLPCN probe development effort in our labs.

Structural Aspects. IDE contains an unusually large internal cavity, uniquely capable of accommodating insulin. Crystal structures of human IDE in co-complex with four substrates were reported in 2006[16]. The Leissring group has also solved IDE-inhibitor co-crystal structures (see PDB Code 3E4A) and found that IDE possesses a number of unusual structural features, including that it must undergo large conformational changes in its catalytic cycle. IDE's unique structure is the key to understanding why IDE inhibitors have remained elusive and also in designing effective new classes of IDE inhibitors.

The overall structure of IDE resembles a clamshell, with two bowl-shaped halves connected by a flexible linker (see **Figure 1** for a schematic diagram highlighting the Zn atom in the active site, and relevant cysteine residues). IDE encapsulates an unusually large (~13,000 Å^3) internal chamber. The co-crystal structure of insulin in complex with IDE[24] revealed that the insulin molecule fits neatly within this cavity, explaining IDE's unique ability to accommodate bulky substrates that make extensive contacts not just with the active site but also with multiple

Figure 1: IDE schematic structure

contact points on the surface of IDE's inner chamber[16]. This unusual feature explains IDE's exquisite substrate specificity, wherein it is the tertiary rather than the primary protein structure of substrates that best determines fit, and also rationalizes IDE's low primary cleavage-site
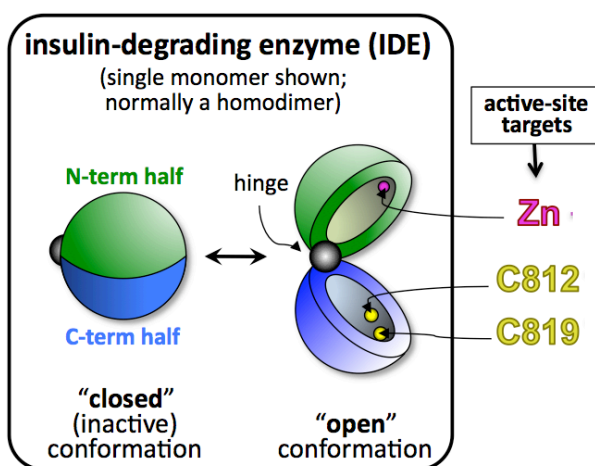
specificity, since interactions distal to the active site will determine the peptide bond that is accessible to the catalytic zinc atom for coordination and eventual cleavage.

Comparison of Tang et al.'s X-Ray crystal structures of IDE[16] to the structure for pitrilysin, a bacterial IDE homolog, suggests that IDE can switch between its "open" and "closed" states[8] (**Figure 2**). Tan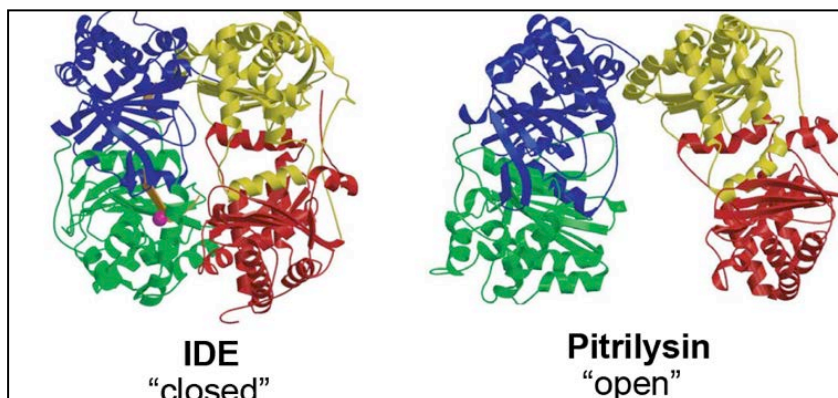g et al. also showed that the activity of IDE can be controlled by engineering a disulfide bridge connecting the two halves, preventing the protease from opening[16].

Figure 2: IDE closed state, and open form of Pitrilysin

Enzymatic analysis of these mutants showed them to be inactive under oxidizing conditions yet active under reducing conditions, providing direct evidence that the protease must switch between open and closed states to complete a catalytic cycle[16].

The finding that IDE is a thiol-sensitive protease distinguishes it from most conventional zinc-metalloproteases. Indeed, IDE was initially classified as a cysteine protease by the Enzyme Commission. The Leissring group elucidated the precise molecular basis underlying IDE's thiol sensitivity[25] through a comprehensive analysis of the 13 cysteine residues in IDE. Cys819 and, to a lesser extent, Cys812, are the principal mediators of this effect. Somewhat counter-intuitively, the cysteine residues that mediate IDE's thiol-sensitivity reside within the C-terminal half of the protease (IDE-C), ~700 amino acids distal to the zinc-binding motif within its N-terminal half (IDE-N) (His108-His112). These results illustrate that IDE's active site is actually bipartite.

Zn site-acting IDE inhibitors act as latches, holding IDE in the closed conformation. While no suitable small molecules are effective IDE inhibitors, larger peptide hydroxamic acid inhibitors act at the zinc site, as shown by a co-crystal structure of IDE and inhibitor Ii1[5]. This peptide hydroxamic acid binds not only to residues within IDE-N, which contains the active-site Zn atom, but also to numerous residues within IDE-C that comprise the second half of IDE's bipartite active site[5]. Ii1 thus spans the active site of the protease, latching it in the closed conformation. It is reasonable to conclude that early failures to identify effective IDE inhibitors through HTS efforts owe to the fact that the screening libraries used had only small molecules (molecular weight <500) incapable of spanning the active site in this manner, *i.e.,* unable to form interactions with both halves of IDE's bipartite active site simultaneously.

Our uHTS campaign was designed to identify IDE inhibitors that target any part of the protein, including the zinc site. Given that the MLSMR library is mostly comprised of small molecules, however, we anticipated that compounds binding by other modes were more likely to arise. Compounds showing IDE inhibition by acting at allosteric sites (though such sites are not yet known to exist for IDE) would be particularly interesting. Also of interest are small molecules that bind near to, or that even covalently modify, one of the crucial cysteine residues, particularly if they are specific for one cysteine residue of IDE and if, moreover, they are also

IDE-selective. Allosteric and cysteine-binding modes for IDE inhibition might not require a large inhibitor to be present in order to achieve a high level of inhibition.

Our uHTS effort was complemented by a focused follow-up and SAR strategy and biochemical strategy to define mode of action, a coordinated effort that has successfully delivered the first potent and selective IDE inhibitor molecular probe, ML345.

2 Materials and Methods

Chemistry: All chemical reagents and solvents were acquired from commercial vendors. Reactions were monitored by LC/MS (Thermo/Finnegan LCQ Duo system with MS/MS capability). An Agilent 1200 analytical HPLC was used for quantitative purity assessment. Teledyne-Isco "combiflash" automated silica gel MPLC instruments were used for chromatographic purifications. A 400 Brüker MHz NMR instrument was used for NMR analysis.

Biology: All protocols are reported in the relevant PubChem AIDs, provided below.

Compound Properties: Solubility, stability, and glutathione reactivity analyses were conducted in accordance with NIH guidelines. CYP450 inhibition and microsome stability analyses were performed as previously described[26].

2.1 Assays

Stage	Assay Type	# Tested	# Active	PubChem AID
	Table 1 IDE Inhibitor PubChem AIDs (click on hyperlink for details). Assay descriptions follow.			
HTS Scripps: MLSMR Liquids	Primary Assay (1X%INH)	324,858	1,316	434962
	Confirmation Assay (3X%INH)	1,179	598	435028
	HEK CYTOX Counterscreen (3X%INH)	1,179	334	449730
	Dose Response (3XIC50)	127	44	463220
	HEK CYTOX Dose Response Counterscreen (3XIC50)	127	1	463221
SAR Scripps: powders (Rounds 0 + 1)	Dose Response (3XIC50)	32	7	588712
	HEK CYTOX Dose Response Counterscreen (3XCC50)	32	2	588709
	Cell-free Wildtype IDE Assay (FP) (3XIC50)	32	9	588711
	Artifact FL Profiling Counterscreen (3XIC50)	32	1	588718
SAR Leissring Lab: powders (Rounds 1 + 2)	Insulin Degradation Assay (3XIC50) Round 1	17	3	624065
	QFRET FRET1 Artifact Assay Round 1	55	10	624066
	WT IDE Cell-free Assay (FP FABB) (3XIC50) Round 1	6	6	624067
	Mutant IDE Cell-free Assay (FRET1) (3XIC50) Round 1	13	2	624306
	Mutant IDE Cell-free Assay (FRET1) (3XIC50) Round 2	26	0	624338
	QFRET FRET1 Artifact Assay Round 2	26	1	624340
	WT IDE Cell-free Assay (FP FABB) (3XIC50) Round 2	26	3	624353

Primary Assay, IDE Inhibition (AID 434962, AID 435028, AID 463220, AID 588712)

The purpose of this assay is to determine the ability of test compounds to inhibit endogenous cellular IDE activity by measuring shifts in the proportion of intact and cleaved forms of the IDE substrate Aβ. This fluorescence polarization (FP)-based assay employs a derivatized Abeta- peptide [Fluorescein-Abeta-(1-40)-Lys-Biotin (FAbetaB)]. Cleavage of FAbetaB by IDE (provided by live HEK cells in the reaction) separates the Fluorescein moiety from the biotinylated moiety. Subsequent addition of avidin to the reaction increases the effective molecular weight of intact, biotinylated FAbetaB substrate, slowing their rotation rate and reducing the degree of depolarization of plane polarized light. In contrast, cleaved FAbetaB substrate species have their Fluorescein moiety separated from the rest of the molecule, which has a low molecular weight, hence rotating rapidly and causing strong depolarization. Thus, the relative amounts of cleaved and intact forms of the FAbetaB substrate can be measured. As designed, compounds that act as IDE inhibitors will inhibit FAbeta-B cleavage, resulting in a population of large avidin-bound, slowly rotating FAbeta-B molecules. Compounds are tested in triplicate at a nominal concentration of 5.59 micromolar.

Secondary Assay #1, HEK Counterscreen (AID 449730, AID 463221, AID 588709)

The purpose of this assay is to determine whether compounds identified as active in the high throughput primary assay to identify inhibitors of insulin-degrading enzyme are nonselective due to HEK cytotoxicity. In this assay, HEK cells are incubated with test compounds, followed by determination of cell viability. The assay utilizes the CellTiter-Glo luminescent reagent to measure intracellular ATP in viable cells. Luciferase present in the reagent catalyzes the oxidation of beetle luciferin to oxyluciferin and light in the presence of cellular ATP. Well luminescence is directly proportional to ATP levels and cell viability. As designed, compounds that reduce cell viability will reduce ATP levels, luciferin oxidation and light production, resulting in decreased well luminescence. Compounds are tested in triplicate using a 10-point 1:3 dilution series starting at a nominal test concentration of 56 micromolar.

Secondary Assay #2, Biochemical Assay for IDE Inhibition (AID 688711, AID 624067)

The purpose of this biochemical assay is to determine whether compounds act directly on IDE. This assay uses the FP-format as used in the Primary Assay, but is cell-free and employs recombinant IDE. Briefly, a range of concentrations of candidate inhibitors were incubated with 2 nM recombinant IDE and 100 nM FabB, and hydrolysis assessed by FP. Compounds that effectively inhibit recombinant IDE will thereby be shown to have a definitive mechanism of action. Compounds that do not inhibit in this assay act by another mechanism. If such compounds are of interest, downstream experiments are to be conducted in the laboratory of the assay provider to elucidate mechanism of action.

Secondary Assay #3, Biochemical Assay for Inhibition of a cysteine-free IDE mutant (AID 624306, AID 624338)

The purpose of this assay is to identify compounds that inhibit IDE activity via thiol-alkylation. This assay also uses an FP-format, but is cell-free and employs a cysteine-free mutant of recombinant IDE. In this assay, compounds that inhibit IDE *via* thiol alkylation in the wild-type enzyme will be ineffective at inhibiting the cysteine free mutant, thereby identifying

them as thiol-alkylating agents. Non-covalent probes are likely to be active in inhibiting cysteine-free IDE. Covalent-acting thiol-modifying compounds should be inactive in inhibiting cysteine-free IDE. Inhibitors of either type are of interest. Identification of mode of action will guide studies intended to define probe selectivity.

Secondary Assay #4, Fluorescence Artifact Assay (AID 588718, AID 624353)

The purpose of this assay is to determine whether powder samples of compounds identified as possible IDE inhibitor probe candidates are nonselective due to their optical activity or fluorescence properties. This fluorescence polarization (FP)-based assay employs a derivatized Abeta- peptide [Fluorescein-Abeta-(1-40)-Lys-Biotin (FAbetaB)]. Cleavage of FAbetaB by IDE separates the Fluorescein moiety from the biotinylated moiety. Subsequent addition of avidin to the reaction increases the effective molecular weight of intact, biotinylated FAbetaB substrate, slowing their rotation rate and reducing the degree of depolarization of plane polarized light. In contrast, cleaved FAbetaB substrate species have their Fluorescein moiety separated from the rest of the molecule, which has a low molecular weight, hence rotating rapidly and causing strong depolarization. Thus, the relative amounts of cleaved and intact forms of the FAbetaB substrate can be measured. As designed, compounds that act as IDE inhibitors will inhibit FAbetaB cleavage, resulting in a population of large avidin-bound, slowly rotating FAbetaB molecules. Quenchers and fluorescent compounds may interfere with the fluorescence polarization readout and appear as inhibiting IDE. In order to identify such assay artifact, tests compounds are added at the end of the reaction, just before measuring fluorescence polarization, so the calculated %inhibition is a result of the optical interference by the compound rather than its impact on IDE activity. Compounds are tested in triplicate using a 10-point 1:3 dilution series starting at a nominal test concentration of 55 µM. The probe was not active in this assay (IC50 value > 55 µM).

Secondary Assay #5, QFRET Fluorescence Artifact Assay (AID 624066, AID 624340)

The purpose of this biochemical assay is to determine whether powder samples of compounds identified as possible IDE inhibitor probe candidates are artifacts due to their interference with the FP assay format. This IDE activity assay differs from the primary FP-based HTS assay (AID 434962). In this assay, a fluorogenic IDE substrate (FRET1) is incubated with wild-type (WT) recombinant IDE in the presence of compounds in reaction buffer. The reaction is monitored by quantification of fluorescence intensity as a function of time. Percent activity is calculated relative to controls containing no experimental compound (100%) or no enzyme (0%). Compounds are tested in triplicate using a 10-point, semilog dilution series starting at a nominal test concentration of 100 µM.

Protocol Summary: Ten microliters of wildtype (WT) recombinant IDE enzyme (1 nM final, i.e., EC80) were dispensed into each well of 384-well microtiter plates, together with control wells loaded with buffer only (Low_Control). Next, 10 µL of test compounds in DMSO (1% final concentration) or DMSO only (High_Control) were added to the appropriate wells. The assay was started by dispensing 10 µL FRET1 substrate (1 µM final) in Buffer A [100 mM NaCl, 10 mM MgCl2, 50 mM HEPES, pH 7.4 supplemented with 0.1% bovine serum albumin (BSA)]. Activity was read continuously at 2 min intervals for 2 h at room temperature (22 C) using a

Molecular Devices SpectraMAX 5e multilabel plate reader (excitation = 335 nm, emission = 385 nm).

For each test compound activity was determined from the rate of increase of fluorescence as a function of time relative to controls, using the linear portion of the progress curves (i.e., 0-30% of complete hydrolysis). For each test compound, percent activity relative to High_Control (100%) was plotted against compound concentration using Microsoft Excel, according to the following formula: %_Activity = 100 * ((Test_Compound - Median_Low_Control) / (Median_High_Control - Median_Low_Control)).   Where:

    Test_Compound indicates wells containing test compound
    Low_Control indicates wells containing Buffer only
    High_Control indicates wells containing DMSO only

The IC50 values were determined by fitting a sigmoidal curve to the data set using Prism 5.0 (GraphPad Software, Inc.) Technologies Inc), solving for the concentration corresponding to 50% activity. In cases where the highest concentration tested (i.e. 100 µM) did not result in greater than 50% inhibition, the IC50 value was determined manually as greater than 100 µM. Compounds with an IC50 value greater than 10 µM were considered inactive. Compounds with an IC50 value equal to or less than 10 µM were considered active. Probe candidates should not exhibit activity in this artifact assay.

Secondary Assay #6, TR-FRET-based IDE activity assay (AID 624065)

The purpose of this biochemical assay is to determine whether powder samples of compounds identified as possible IDE inhibitor probe candidates can inhibit the ability of recombinant IDE to degrade insulin in vitro. This assay is a proximity-based immunoassay that uses two monoclonal antibodies, one labeled with Eu3+-Cryptate and one labeled with XL665 that recognize distinct epitopes on the insulin molecule. Compounds are tested in triplicate using a 10-point semi-log dilution series starting at a nominal test concentration of 100 µM (highest dose).   Details of this assay are available at the manufacturer's website: http://www.htrf.com/products/cns/insulin/

Ten microliters of WT recombinant IDE enzyme (1 nM final, i.e. EC80) were dispensed into each well of 384-well microtiter plates. Next, 10 µL of test compound in DMSO, low control (1% DMSO final concentration), or high control (1 µM IDE inhibitor Ii1) were added to the appropriate wells. To define background fluorescence (background control) a subset of wells were filled with 10 µL buffer only (no insulin). The assay was started by dispensing 10 µL of insulin (100 nM final) in Buffer A [100 mM NaCl, 10 mM MgCl2, 50 mM HEPES, pH 7.4 supplemented with 0.1% bovine serum albumin (BSA)]. Plates were then incubated for various lengths of time at room temp (22 C), then the reactions were terminated by addition of 5 µL of the broad-spectrum zinc-metalloprotease inhibitor 1,10 phenanthroline (2 mM final). TR-FRET was measured using a Molecular Devices SpectraMAX 5e multi-label plate reader (excitation = 337 nm, emission A = 665 nm and emission B: 620 nm, with a 400 ms delay time). Raw TR-FRET values (TRFraw) were determined from the following formula: TRFraw = Em665 / Em620

Next, background-subtracted TR-FRET values (TRFsub) were calculated according to the following formula: TRFsub = TRFraw - Mean_Background_Control_TRFraw

Where: Mean_Background_Control_TRFraw is defined as the raw TR-FRET values obtained in wells containing no insulin. For each test compound, percent activity relative to Low_Control (100%) was plotted against compound concentration using Microsoft Excel, according to the following formula:

100*((Test_Compound - Median_Low_Control) / (Median_High_Control - Median_Low_Control))

Where:
Low_Control is defined as DMSO-treated wells only.
Test_Compound is defined as wells containing test compound.
High_Control is defined as wells containing reference IDE inhibitor Ii1.

Secondary Assay #7, Proteome-wide profiling of cysteine reactivity

The purpose of this assay is to determine if covalent, cysteine-reactive probes measurably affect other cysteine-reactive members of the proteome at doses ranging from 2 nM to 20 μM. The assay is an activity-based protein profiling assay for late-stage analysis of a potential IDE inhibitor probes. Briefly, test compounds are incubated for 30 min at 37 °C, then labeled for 30 minutes with 5 µM chloroacetamide-Rh at 25 °C giving results as shown in Section 3.6.

2.2   Probe Chemical Characterization

The chemical structure of the probe was verified by analysis of its 400 MHz ^{1}H NMR spectra (**Figure 3**) obtained on a Brüker 400 MHz instrument and supported by analysis of a ^{19}F NMR spectrum obtain on the same instrument. The chemical structure was also corroborated by its LC/MS molecular ion (calc for M+1: 480.1, found 479.9, using a Thermo/Finnegan LCQ Duo system). Purity was measured at >98% (LC/MS analysis, confirmed by analytical HLPC analysis; HPLC purity data is shown in **Figure 4**). HPLC data was obtained using an Agilent 1200 analytical HPLC with an Agilent Eclipse XDB-C18 column, 4.6X150mm. The HPLC solvents used were acetonitrile and water with 0.1% formic acid added to each mobile phase as the pH modifier.
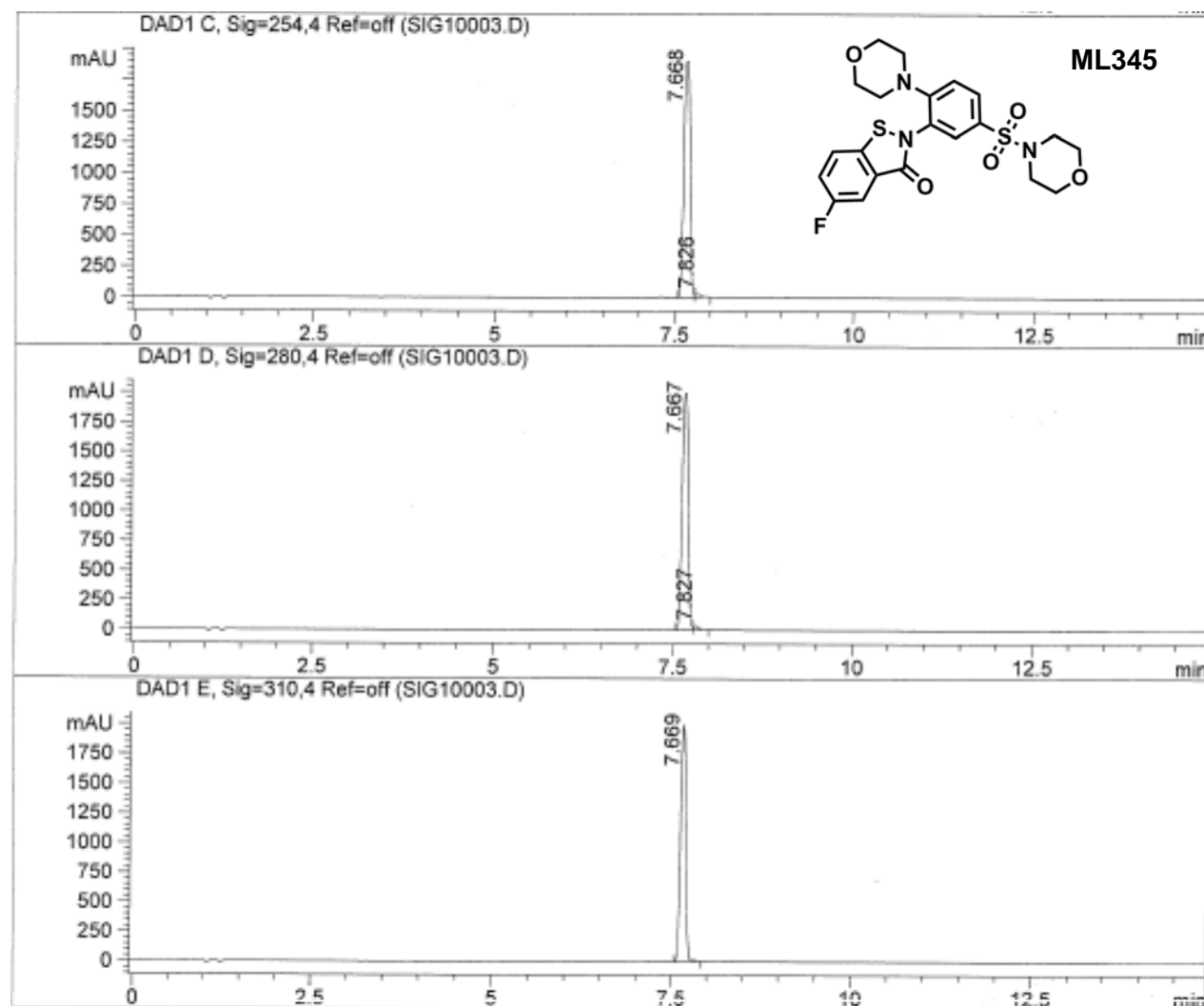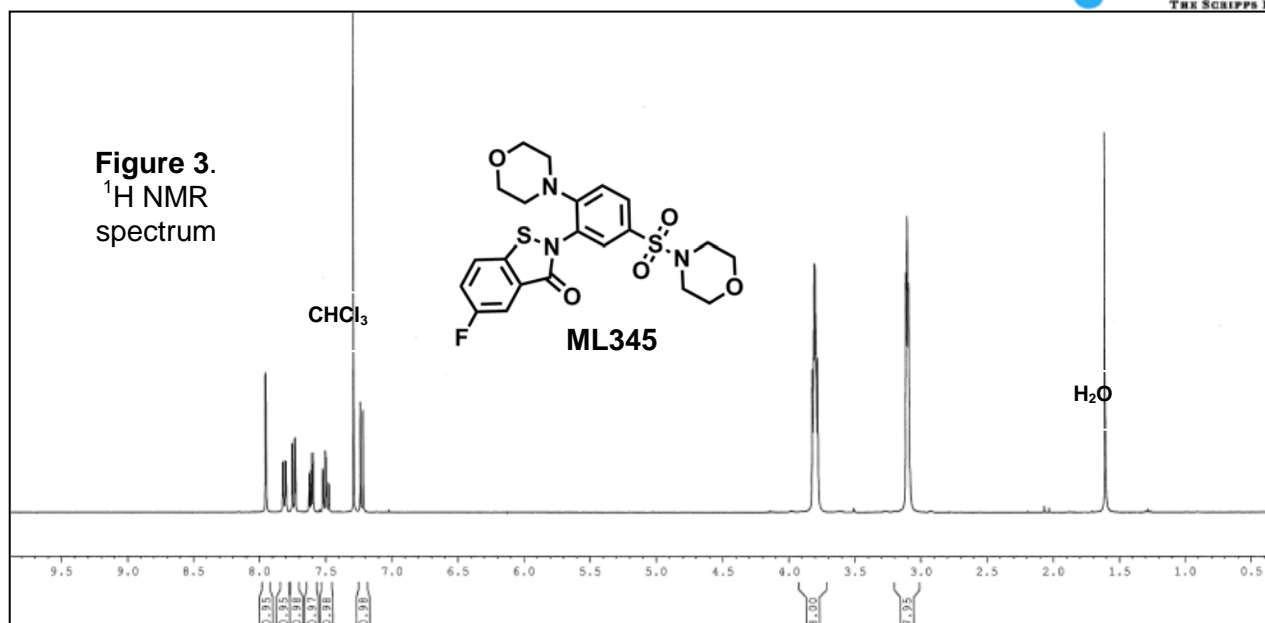
Figure 3. ^{1}H NMR spectrum

Figure 4. HPLC Spectrum of ML345 at various wavelengths; purity >98%

The solubility of the probe in PBS at pH 7.4 was determined to be moderately low (0.4 μM), however, the solubility in simulated general assay buffer (DMEM + FBS) was substantially higher (5.1 μM). Its solubility is fully adequate to provide the high potency seen in cell-based assays. The measured solubility suggests that, when appropriately formulated, the solubility of ML345 is adequate for broad use as a biological probe. The FBS effect could indicate high protein binding, which we did not directly measure.

The probe has a half-life of >>48 hours in PBS at room temperature when tested at 10 μM (**Figure 5**).

Disappearance of the LC peak for the probe is altered slowly but significantly by the addition of excess (50 μM) glutathione, with ~25% erosion of the parent peak
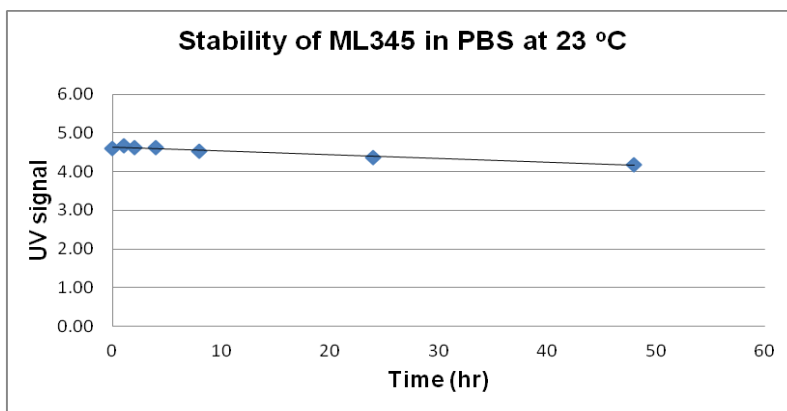
Figure 5. 48 hour stability study of ML345 in PBS

area after 3 hours and ~41% erosion after 6 hours, suggesting a half-life of ~7.5 hours with 10-fold excess glutathione present. This agrees with the expectation that, while ML345 can be made to react with free thiols, it has significant selectivity for IDE, and specifically for reacting with Cys819 of IDE. The probe is stable in DMSO solution at 23°C (no erosion of peak intensity after 7 days) and is also stable as a free base dry powder. It is also stable under assay conditions, as indicated by potency in cell-based assays that is independent of incubation time.

The following compounds have been submitted to the MLSMR (MLS numbers pending):

Table 2. Probe ML345 and Analogs						
Designation	**Structure**	**CID**	**SID**	**SR ID**	**Amount submitted (mg)**	**Date Submitted**
Probe ML345		57390068	144241486	SR-03000002959-2	20	12/17/2012
Analog 1		57390067	144241485	SR-03000002958-2	15	12/17/2012
Analog 2		5295225	144241488	SR-03000003056-1	15	12/17/2012

Analog 3		4317404	144241489	SR-03000003057-1	15	12/17/2012
Analog 4		5023882	144241490	SR-03000003058-1	15	12/17/2012
Analog 5		1510390	144241491	SR-03000003059-1	15	12/17/2012

2.3 Probe Preparation

Overview. The probe ML345 was synthesized in a straightforward fashion in a convergent manner, in six steps overall, with the longest linear sequence being 4 steps, as summarized in **Figure 6**. The overall yield of the process (after preparative HLPC purification of the final product) is 26%. *Analogs for SAR evaluation were prepared by similar methods.*
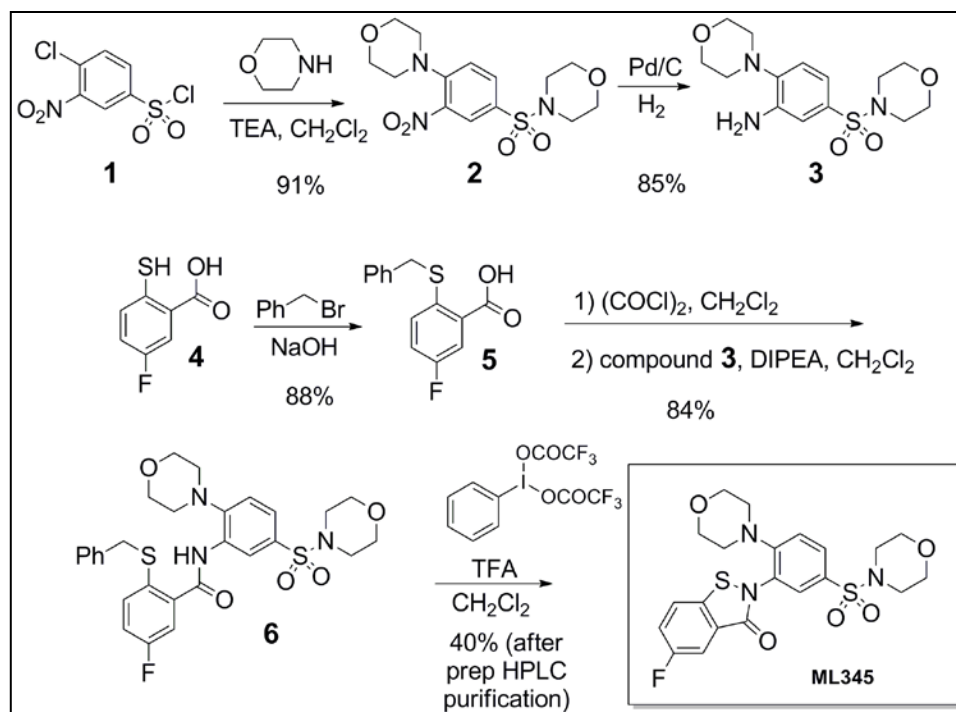
Figure 6. Synthesis of probe ML345

Step 1.
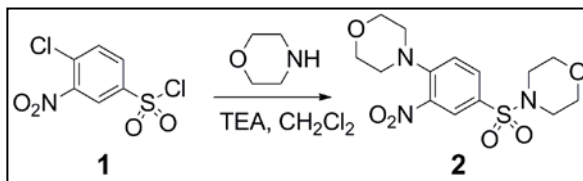
A mixture of acid chloride **1** (2.36 g, 10 mmol) and triethylamine (5.06 g, 50.0 mmol) in CH_2Cl_2 (50 mL) was treated with dropwise with morpholine (2.61g, 30 mmol) at room temperature. After addition was complete the reaction was stirred at room temperature for 14 h, quenched with saturated NH_4Cl, and extracted with ethyl acetate. The combined organic extracts were washed with brine and dried over Na_2SO_4. The solvent was removed and the residue was purified by flash column chromatography (Hexanes: ethyl acetate = 1:1, R_f= 0.15) to afford 3.261 g (91%) of compound **2** as a yellow solid. Calc'd for $C_{14}H_{19}N_3O_6S$: 357.1; found $[M+H]^+$: 358.0; ^{1}H NMR (400 MHz, $CDCl_3$) δ (ppm) 3.03-3.06 (m, 4H), 3.21-3.23 (m, 4H), 3.76-3.79 (m, 4H), 3.87-3.89 (m, 4H), 7.18 (d, J=8.8 Hz, 1H), 7.79 (dd, J=2.0, 8.8 Hz, 1H), 8.17 (d, J=2.0 Hz, 1H).

Step 2.
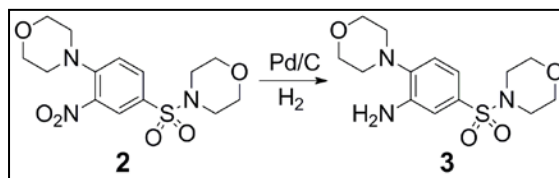
To a solution of compound **2** (488 mg, 1.37 mmol) in THF (10 mL) and MeOH (10 mL) was added Pd/C (10%, 50 mg). The reaction mixture was then stirred under atmosphere of H_2 for 5 h, filtered and concentrated to afford 378 mg (85%) of compound **3** as white solid. Calc'd for $C_{14}H_{21}N_3O_4S$: 327.1; found $[M+H]^+$: 328.1.

Step 3.
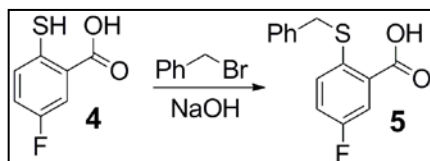
A solution of Acid **4** (344 mg, 2.0 mmol) in MeOH (12 mL) was treated with NaOH (160 mg, 4.0 mmol). The reaction mixture was stirred at room temperature for 10 min. The solvent was removed to afford a solid which was dissolved in acetone (18 mL). Benzyl bromide (376 mg, 2.2 mmol) was added. The reaction was sonicated for 5 min and then stirred at 0 °C for 1 h. The precipitate was collected by vacuum filtration. The solid was dissolved in H_2O and then treated with 1 N HCl. The precipitate was collected by vacuum filtration and dried in air, affording 462 mg (88%) of compound **5** as white solid. ^{1}H NMR (400 MHz, acetone-d_6) δ (ppm) 4.25 (s, 2H), 7.27-7.36 (m, 4H), 7.45-7.47 (m, 2H), 7.54-7.57 (m, 1H), 7.70-7.73 (m, 1H).

Steps 4 and 5.
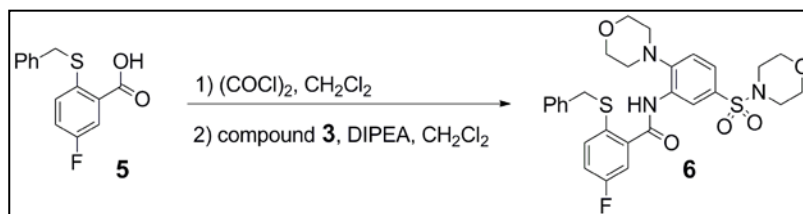
A suspension of acid **5** (570 mg, 2.17 mmol) in CH_2Cl_2 (24 mL) was treated with $(COCl)_2$ (441 mg, 3.48 mmol) and a drop of DMF at 0 °C under atmosphere of N_2. The reaction was stirred at 0 °C for 30 min, and then room temperature for 3 h. The solvent was removed. The residue was dissolved in CH_2Cl_2 (24 mL). Compound **3** (781 mg, 2.39 mmol) was added and cooled to 0 °C. Diisopropylethylamine (841 mg, 6.51 mmol) was added dropwise. The reaction mixture was stirred at room temperature overnight, quenched with H_2O, extracted with CH_2Cl_2. The combined organic extracts were washed with brine, dried over Na_2SO_4. The solvent was removed and the residue was purified by flash column (hexanes: ethyl acetate = 1:1, R_f = 0.20) to afford 1.04 g (84%) of compound **6** as a yellow solid. Calc'd for $C_{28}H_{30}FN_3O_5S_2$: 571.1; found [M+H]$^+$: 572.0;. ^{1}H NMR (400 MHz, $CDCl_3$) δ (ppm) 2.93-2.95 (m, 4H), 3.13-3.15 (m, 4H), 3.78-3.83 (m, 8H), 4.05 (s, 2H), 7.07-7.09 (m, 3H), 7.19-7.20 (m, 3H), 7.30-7.33 (m, 2H), 7.42-7.45 (m, 1H), 7.58-7.60 (m, 2H), 8.92 (br s, 1H); ^{19}F NMR (400 MHz, $CDCl_3$) δ (ppm) -111.6.

Step 6.
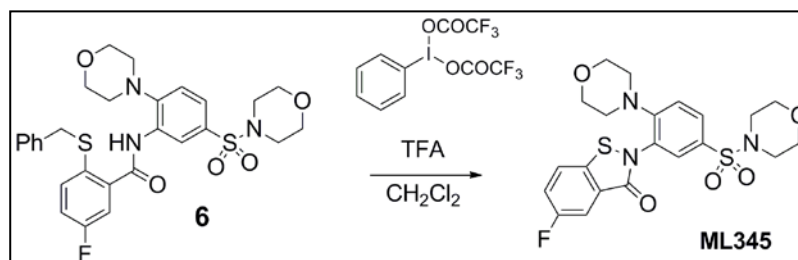
A mixture of [bis(trifluoroacetoxy)iodo]benzene (PIFA, 1.02 g, 2.36 mmol) and TFA (0.415 g, 3.64 mmol) in CH_2Cl_2 (18 mL) was cooled to 0 °C under atmosphere of N_2. A solution of compound **6** (1.04 g, 1.82 mmol) in CH_2Cl_2 (35 mL) was added dropwise. The reaction mixture was stirred at 0 °C for 30 min, room temperature 30 min, and then refluxed for 40 h. The crude product was concentrated and the residue was purified by flash column chromatography (hexanes : ethyl acetate = a gradient of 1:1 to 1:4) and then by preparative HPLC to afford 343 mg (40%) of ML345 as a white solid. Calc'd for M+H = $C_{21}H_{23}FN_3O_5S_2$: 480.1; found [M+H]$^+$: 479.9; ^{1}H NMR (400 MHz, $CDCl_3$) δ (ppm) 2.98-3.01 (m, 8H), 3.67-3.71 (m, 8H), 7.11 (d, J=8.8 Hz, 1H), 7.36-7.41 (m, 1H), 7.48-7.52 (m, 1H), 7.63 (dd, J=2.4, 8.4 Hz, 1H), 7.70 (dd, J=2.4, 8.0 Hz, 1H), 7.84 (d, J=2.0 Hz, 1H); ^{19}F NMR (400 MHz, $CDCl_3$) δ (ppm) -115.4.

3   Results

3.1 Summary of Screening Results

An overall sum-mary of the screening campaign in shown in **Figure 7**. Briefly, uHTS primary screening of ~325,000 compounds gave 1,316 primary IDE INH hits. Counterscreening for toxicity and for (artifact) fluorescence interference gave 139 hits of highest interest. 127 available com-pounds were profiled in dose-response format for cell-based IDE activity and a total of 43 non-toxic compounds were then considered for follow-up testing of independent, freshly prepared powder samples by the SRIMSC. All results are available in PubChem using the indicated AIDs.

The series of efforts used to select probe candidate scaffolds and ultimately to identify molecular probes is summarized in the general hit-to-probe optimization flow chart (**Figure 8**). Chemistry and cheminformatics-based analyses of the results of the μHTS campaign allow for reactive, non-selective, assay-promiscuous, and otherwise non-tractable hits to be removed from further consideration.

Following these analyses, the most tractable compounds are ordered through for confirmation screening of a second batch. Any non-repeating samples are ignored for further probe development, as are compounds lacking targeted activity in secondary assays.
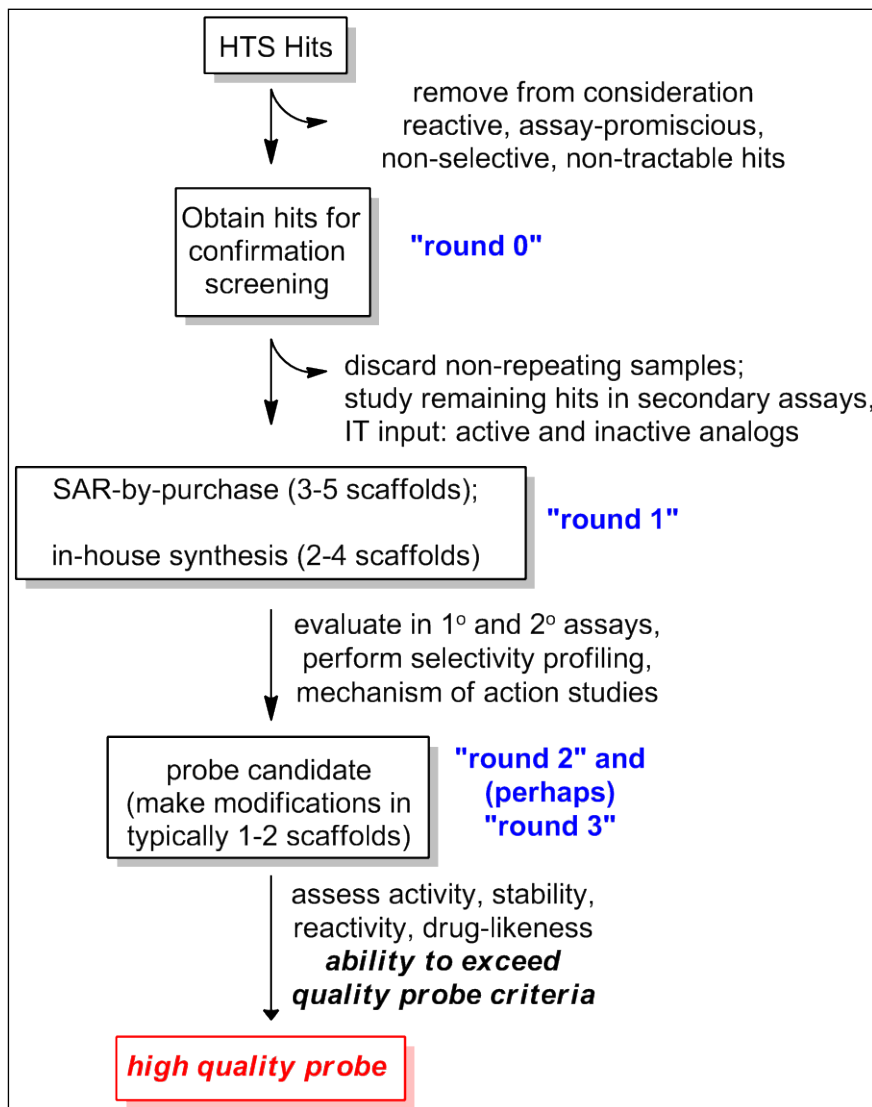

Figure 7. Screening campaign overview
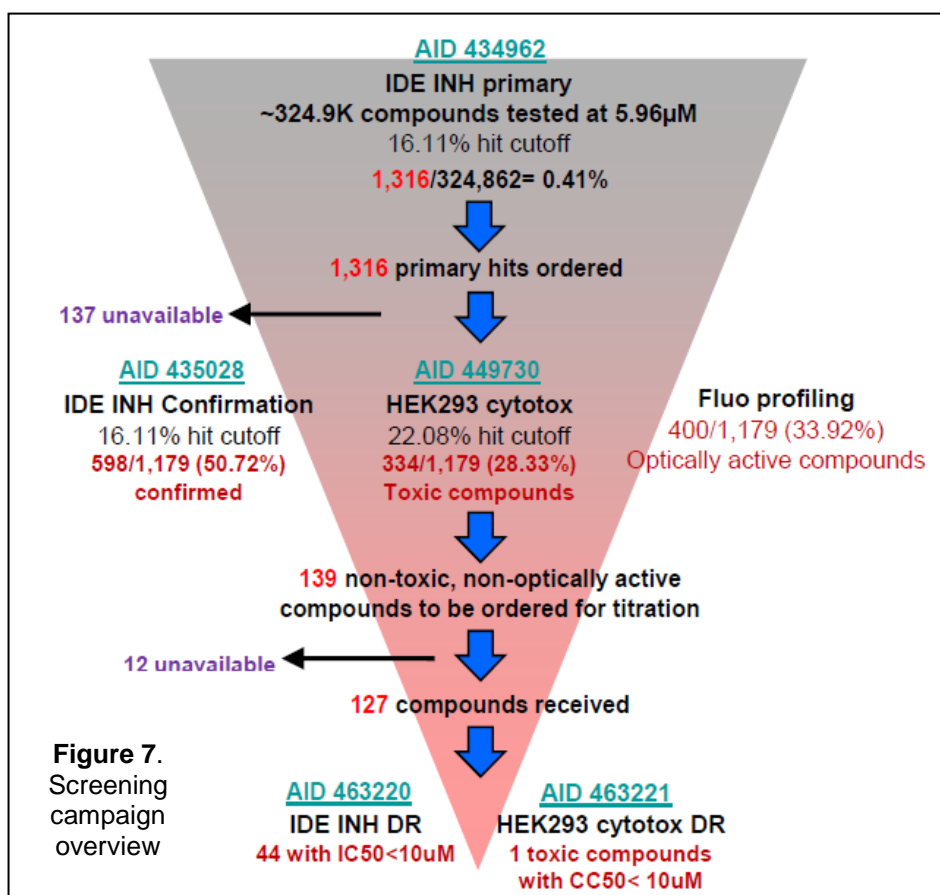
Confirmed hits then allow for selection of scaffolds for probe development, aided by computational analysis of active and inactive analogs from the uHTS effort, to gauge potential of scaffolds to have meaningful non-flat SAR. Iterative rounds of medicinal chemistry and SAR development, complemented by assessment of compound properties, aids in selection of a high-quality probe.

The most interesting IDE screening hits are shown in **Table 3** below. The screening hit selection criteria include structural desirability, high potency in IDE Inhibition dose-response (cell-based EC_{50} <10 µM), high maximal degree of inhibition (>75%), and lack of activity in the HEK toxicity and fluorescence artifact counterscreens (toxic and non-selective agents were excluded from probe development consideration).

Each of the compounds shown in **Table 3** also displayed IDE activity when an independent batch was assayed (these "powder confirmation" EC_{50} values were within 2-fold of the uHTS result). All new batches of compounds were also inactive in the HEK toxicity counter-screen and also in the fluorescence artifact counterscreens (EC_{50} or IC_{50} in each case >>10 µM).

Figure 8. Probe development strategy, post-uHTS

HTS Hits

remove from consideration reactive, assay-promiscous, non-selective, non-tractable hits

Obtain hits for confirmation screening **"round 0"**

discard non-repeating samples; study remaining hits in secondary assays, IT input: active and inactive analogs

SAR-by-purchase (3-5 scaffolds);

in-house synthesis (2-4 scaffolds) **"round 1"**

evaluate in 1° and 2° assays, perform selectivity profiling, mechanism of action studies

probe candidate (make modifications in typically 1-2 scaffolds) **"round 2" and (perhaps) "round 3"**

assess activity, stability, reactivity, drug-likeness *ability to exceed quality probe criteria*

high quality probe

Our initial focus was upon three scaffolds shown in the middle of **Table 3**:
- triazoles (CIDs 667188 and 664941),
- the thiazole amide CID 1483690, and
- the diacylpiperazine CID 17583130.

Analogs in each series are synthetically readily accessible. Further, literature analysis suggested that each series was tractable. We also preferred hits that were expected to be non-covalent inhibitors. Nine close structural analogs of the triazole CID667188 were prepared. However, seven of these analogs were found to be completely *inactive vs.* IDE, while the remaining two compounds were *less potent* than were the original hits. Even minor structural

changes tended to eliminate all IDE activity. Poor water solubility was also a concern in the triazole series (*e.g.;* the cLogP for CID667188 is ~5.0). For these reasons, non-triazole probe development scaffolds were instead pursued. Seven structural analogs of the thiazole amide CID 1483690 were prepared and all were found to be completely inactive *vs.* IDE, prompting us to also discontinue efforts in this chemical series.
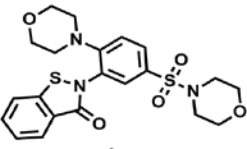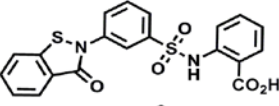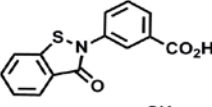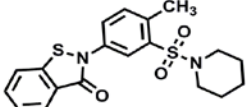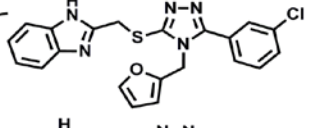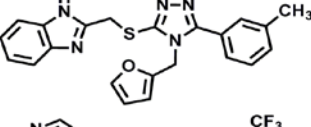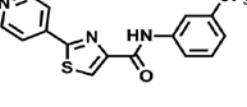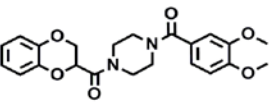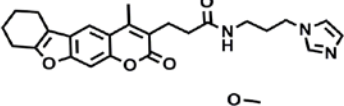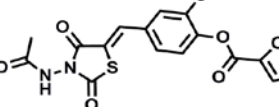
Structure	Pubchem CID	Pubchem SID	IDE EC$_{50}$ HTS (µM)	max response	Activity promiscuity analysis: active / total
	2325815	24840227	1.4	108	56 / 487 11.5%
	4089709	49724792	2.1	113	31 / 208 14.9%
	25181200	25181200	2.4	106	9 / 103 8.7%
	2327953	24840413	4.0	100	69 / 521 13.2%
	667188	865930	2.6	106	8 / 488 1.6%
	664941	863688	5.7	98	13 / 496 2.6%
	1483690	24818077	5.3	76	3 /328 0.9%
	17583130	49825176	1.2	85	2/268 0.7%
	4869155	49822462	4.3	107	5 / 211 2.4%
	2574532	85271396	5.8	127	5 / 95 5.3%

(hits of highest initial interest — bracket spanning CID 667188 through 17583130)

Table 3. Hit summary, promiscuity analysis (reflects PubChem data available at time of uHTS).

We then focused our attention upon the diacylpiperazine CID 17583130, initially encouraged by the simple tractable structure, IDE inhibitory activity of this compound, and by similar potency observed for several selected analogs that were purchased from a commercial vendor. However, when a sample of CID 17583130 was prepared internally (SID 124756577), this analytically pure sample was *completely inactive vs. IDE* (EC$_{50}$ >100 µM). HPLC traces showed that the internally-generated sample was essentially identical in composition, at least by UV absorption, to both purchased samples of the "same" compound (SID 49825176 and SID 117689475). 21 structural analogs of CID 17583130, prepared internally in high purity, were also found to be inactive, though several purchased analogs were at least weakly active. When the purchased (previously active!) sample of CID 17583130 was rigorously purified by preparative HPLC (given SID 134420263 after purification), *all IDE inhibitory activity was lost.*

The above series of observations indicates that a non-organic and non-UV-active impurity is responsible for the IDE inhibition observed for batches of diacylpiperazines tested as purchased, without purification, samples that nevertheless had passed LCMS purity criteria owing to the absence of secondary peaks in the UV spectrum. We feel that this disappointing series of false positive results is likely due to the high sensitivity of the zinc or thiol moieties in IDE toward trace impurities that were present in the commercial samples as obtained from the vendor. Efforts to identify the active impurity or impurities have been unsuccessful. Thus the diacylpiperazine series was also eliminated from further consideration as a probe class.

The two hits shown at the bottom of **Table 3**, CID 4869155 and CID 2574532, were also eliminated from consideration for follow-up due to undesirable properties. Specifically, the high molecular weight and high LogP of CID 4869155, as well as the lack of active analogs in the uHTS collection, were concerns. The rhodanine-like hit CID 2574532 was also considered undesirable for chemical tractability reasons.

We expected that the four compounds shown at the top of **Table 3**, in a structural class termed the benzoisothiazolidones, were acting as *covalent reversible modifiers of a cysteine residue* at the active site of IDE through the formation of a disulfide bond. This feature distinguishes the class from the other entries in **Table 3**, which were expected to be *non-covalent* inhibitors, but that had, in every instance, proved ill-suited for probe development. This proposed mechanism of action for inhibition by the benzoisothia-zolidones is illustrated in **Figure 9**.
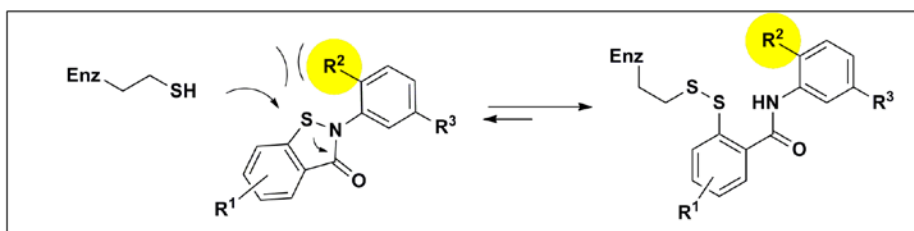

Figure 9. Benzoisothiazolones target a cysteine residue of IDE

Notably, the most potent HTS hit, CID 2325815 (top entry in **Table 3**) has a morpholine group present at the R^2 position (see the highlighted R^2 group depicted in **Figure 9**). Were these benzoisothiazolidone inhibitors merely acting as non-selective and chemically reactive "traps" for a cysteine residue, without significant cooperative binding to the enzyme, such a bulky and electron-donating R^2 group would be expected to instead *decrease* the ability of the

ligand in interact with IDE. Further, we found non-flat SAR found in this series, first as determined by cheminformatics analysis of uHTS results (percent IDE inhibition results for structural analogs of CID 2325815 that were present in the screening collection), and then verified by dose-response studies of several of these analogs (SAR data is shown later in section 2.4). These two lines of evidence suggested that there would be a high potential for finding a potent and selective IDE inhibitor probe in the benzoisothiazolidone scaffold.

When a freshly prepared second sample of CID 2325815 was obtained (SID 104144357) this analytically pure powder confirmation sample nearly duplicated the uHTS cell-based results, as shown in **Figure 10**, with EC_{50} ~2 μM (green curve, comparable with EC_{50} = 1.4 μM found for SID 24840227 in the uHTS campaign). Moreover, we saw promisingly high potency in an IDE biochemical assay (IC_{50} ~600 nM, black curve). Further, no HEK toxicity was seen at any dose (red curve) and no artifact fluorescence interference was seen below 10 μM (blue curve). *This favorable profile supported the selection of the benzoisothiazolidones as a probe series.*

Figure 10. Profile of most potent uHTS hit, CID 2325815. Data is for SID 104144357.
Black = cell-free IDE assay
Green = cell-based IDE assay
Blue = autofluorescence assay
Red = HEK toxicity assay
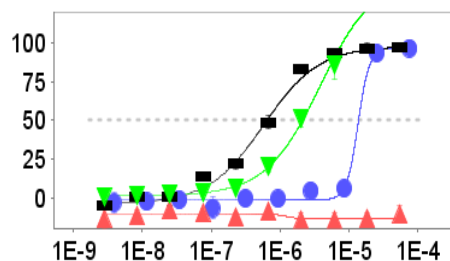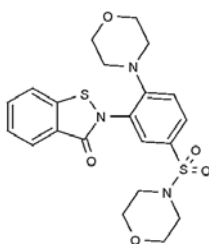
The use of covalent modifiers as molecular probes, and even as drugs, has been an area of considerable interest and substantial ongoing debate[27]. The stable covalent complex can confer favorable properties associated with long target residence time. Selectivity for the target in question (in this instance IDE) over other members of the proteome having reactive cysteine residues is of higher concern, however. A second concern is possible immunogenic effects of a covalently modified protein target, though this concern is lessened when the covalent modification is reversible, as in the case of benzoisothiazolidones. Our initial probe development plan expressed a preference for development a non-covalent probe, for the reasons listed above. In this case, however, we were thwarted by repeated difficulty in finding non-covalent hits that were not assay artifacts.

Keeping the concerns over covalent modifiers in mind, while also factoring in the potency, counterscreen selectivity, and high maximal inhibition seen in the benzothiazolidone class (see **Figure 10** above) we chose this series for probe optimization. We ultimately identified even more potent IDE inhibitors (shown later in section 3.4, SAR table) and found a probe with suitable target selectivity and potency, the declared probe ML345, a fluorinated analog of the screening hit CID 2325815 (**Figure 11**).
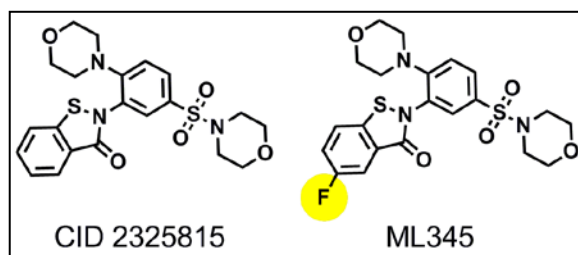

Figure 11. ML345 is a fluorinated analog of CID 2325815

3.2 Dose-Response Curves for Probe

We found that other benzoisothiazolones that are related to the screening hit CID 2325815 maintain the same general profile shown above in **Figure 10**: highest potency in the biochemical assay, followed by the cell-based IDE assay, with minimal autofluoresence at inhibitory levels, and no inherent toxicity in the HEK counterscreen.

The IDE inhibition curves are shifted to the left when the benzoisothiazolone ring bears an appropriately-positioned electron withdrawing group, consistent with the covalent reactivity of the probe as discussed earlier and depicted in **Figure 9**. **Figure 12** below shows the inhibition curve for ML347 in the biochemical (cell-free) assay, using DTT-free, wild-type, recombinant IDE. The IC_{50} measured in the Leissring lab was 188 nM (SID 136920229). When a larger, equally pure probe batch was tested at a later date (SID 144241486), its IC_{50} was measured at 1.1 µM. This slight discrepancy may be due to a variation in activity of different batches of IDE used in each assays (positive controls were also higher in the latter run). The IDE enzyme is quite sensitive to handling and purification methods, showing significant batch-to-batch variability. The lower-end values for the probe (~200 nM) are more typical and (we feel) more accurate, particularly considering the positive control was on outlier in the experiment giving the higher IC_{50} value.   Nevertheless, the probe is a potent IDE inhibitor in biochemical assays, is only active vs. native IDE and not a mutant form lacking Cys819, and is a significant advance in the field given the absence of small molecule prior art.
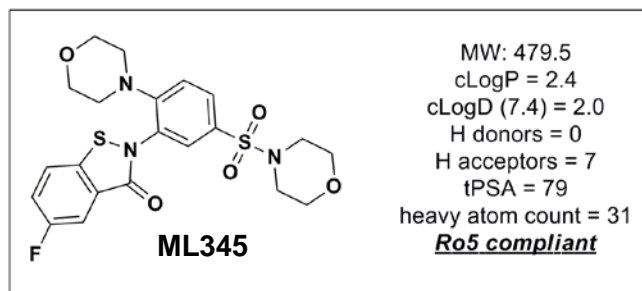
Figure 12. Probe dose-response curve, IDE inhibition (AID 624065, SID 136920229)
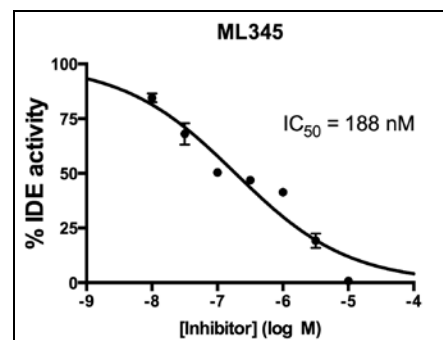
3.3 Scaffold/Moiety Chemical Liabilities

We have calculated various chemical descriptors for the probe using the Accelrys Pipeline Pilot software and by applying standard "rule-of-five" and other lead-likeness or drug-likeness criteria[28-30]. As shown in **Figure 13** below, all calculated parameters meet these criteria. The probe has a moderately cLogP and modestly high polar surface area, with suitable molecular weight, H-bond donor/acceptor counts, and with *no significant structural-based concerns from a stability, lead-likeness, drug-likeness, or general toxicity alert[31] perspective.*

Figure 13. Lipiniski and other drug-likeness parameters for ML345

MW: 479.5
cLogP = 2.4
cLogD (7.4) = 2.0
H donors = 0
H acceptors = 7
tPSA = 79
heavy atom count = 31
Ro5 compliant

ML345

The calculated partition coefficients shown in **Figure 13** for ML345 (*e.g.,* LogD$_{7.4}$ = 2.0) suggests the potential for significant aqueous solubility that could aid its utility as a probe. As was described earlier, the solubility of the probe in PBS was somewhat lower than anticipated, 0.4 μM. The solubility in simulated general assay buffer was more reasonable (5.1 μM) suggesting that formulation strategies, with solubilizing additives, should be considered by researchers using the probe. Also, as shown earlier (**Figure 5**), the probe is chemically stable in a PBS solution: neither a substantial erosion of parent LCMS peak intensity nor an emergence of new peaks was seen over a 48-hour study.

The potential for biological stability was assessed by incubation of the probe with hepatic microsome preparations (1 mg/mL) using known methods[26]. The probe is highly stable to liver microsomes, with a measured half-life of >120 minutes (human liver microsomes), 24 minutes (mouse microsomes), and 50 min (rat microsomes). High hepatic microsome stability is consistent with attributes of a compound intended to be used in the study of relevant *in vivo* effects.

Inhibition of cytochrome P450 enzymes (CYPs) is a marker for drug-drug interaction potential. An *in vitro* study used four relevant CYP isoforms (1A2, 2C9, 2D6, and 3A4). The appropriate positive controls, compounds known to inhibit individual CYP isoforms (furafylline, sulfaphenazole, quinidine, and ketoconazole), were used.[26] The analysis, shown in **Table 4**, determined that ML345 inhibits these CYP isoenzymes between 57-94% at 10 μM. This suggests that ML345 requires significant improvements with regard to CYP450 inhibition profile for safe use therapeutically; however, its profile should not hinder the utility of ML345 as a molecular probe and biological tool compound to study the importance of IDE, especially since it is a first-in-class small molecule inhibitor of IDE.

Table 4: CYP450 Inhibition of Probe ML345

Compound ID	Inhibition of CYP1A2	Inhibition of CYP2C9	Inhibition of CYP2D6	Inhibition of CYP3A4
ML345 (10 μM)	81% (Furafylline standard @40 μM)= 86%)	75% (Sulfaphenazole standard @10 μM)= 93%)	57% Quinidine standard @10 μM)= 90%	94% (Ketoconazole standard @1 μM)= 94%)

The selection of a covalently-reactive probe series, as discussed previously, demanded that we clearly show that the probe does not behave simply as a broadly reactive and non-selective cysteine trap. We have compiled several lines of evidence, including non-flat SAR (shown later SAR discussed later in Section 3.4) and profiling assays (discussed later in Section 3.6) to show that the probe has suitable target selectivity to be useful as a molecular probe.

The probe scaffold is termed a benzoisothiazolidone. We are not aware of any undesirable attributes of the scaffold, other than potential reactivity with cysteine-containing proteins (an issued addressed in Section 3.6, assay profiling) and the CYP450 inhibition we have observed, which is likely compound-specific rather than scaffold-specific. While *in vivo* studies are beyond the scope of the probe development effort, the electron-deficient aryl groups present in ML345 would tend to protect it from susceptibility to rapid oxidative metabolism. The sulfonamide group of ML345 is not normally prone to redox issues. The aniline moiety present is tri-substituted, sterically hindered, and electronically deactivated, thus this group is also unlikely to contribute to potential metabolic liabilities for the probe.

The relative ease of synthesis of the probe molecule and analogs by a convergent six step sequence (4 linear steps) in a reasonable yield (see **Figure 6** in Section 2.3) is a strong asset for this scaffold and for this probe. Scale-up synthesis, if needed for extensive long-term studies, will be highly feasible.

An MLPCN probe with the benzoisothiazolidone scaffold has already been approved. This compound, ML089, is a potent, selective, and orally bioavailable phosphomannose isomerase inhibitor (IC$_{50}$ = 1.3 μM)[32]. This same compound (entry 3 in **Table 5**, shown later in Section 3.4) is also an IDE inhibitor, though it is ~20-fold less potent *vs.* IDE than is ML345. Very importantly, however, the reported highly favorable DMPK properties of ML089, including high oral bioavailability[32], support the assertion that analogs tailored for potent and selective IDE inhibition may also have similarly favorable DMPK properties.
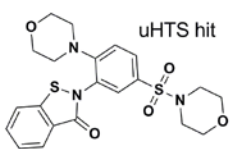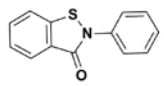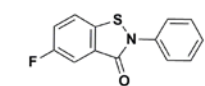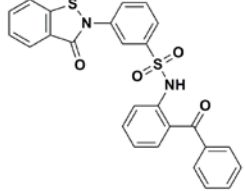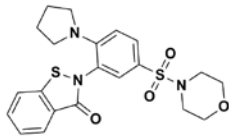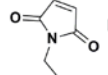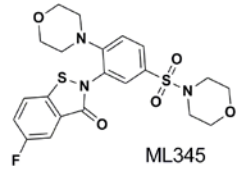

Table 5. Abbreviated SAR summary in the probe scaffold showing cell-free (biochemical) results.

3.4   SAR Tables

After the team selected CID 2835215 as a probe development scaffold, we investigated structure-activity relationships (SAR) of the series that were apparent from uHTS results, since several related compounds were in the MLSMR library and had been screened.   We also analyzed SAR of purchased analogs as well as related inhibitors synthesized internally. IDE inhibitory activity was measured in triplicate, using the cell-free IDE inhibition assay, and selected results are shown above in **Table 5** (values for three other analogs present in the uHTS are shown in Table 3 and are not duplicated here). The screening hit and the eventual probe ML345 are shown at the top (entry 1) and bottom (entry 7) of **Table 5**, respectively, for comparison.

Briefly, entry 1 (the uHTS hit) has suitable activity for SAR development (The Scripps IC_{50} value was ~600 nM, as shown earlier in **Figure 10**, with EC_{50} in the cell-based assay = 1.4 μM; values shown in **Table 5** are from the cell-free assay, measured in the Leissring lab).

Entry 2 shows that deletion of both the morpholine and morpholine sulfonamide groups present in the uHTS hit diminishes IDE activity more than 10-fold, suggesting that both of these groups play a role in IDE recognition.

Entries 3 and 4 show that electron withdrawing groups in either aryl ring enhances IDE inhibition (compare with entry 2).

Entry 5 shows that a pyrrolidine ring is less well-tolerated than is the morpholine ring present in the uHTS hit, again suggesting that morpholine group plays a important role in IDE recognition.

Entry 6 shows the very weak activity of a prototypical non-selective covalent "cysteine trap" N-ethyl maleimide.

Finally, the probe compound ML345 is shown in entry 7, which, like entry 3, bears a *para*-fluorine substituent to further augment IDE inhibitory activity (as suggested by entry 3). IDE inhibition is also aided by the presence of the morpholine ring and the sulfonamide group (as suggested by entries 3 and 4).

We draw another important conclusion from analysis of **Table 5**: *the SAR in the benzoisothiazolidone series is not flat*, *i.e.;* all compounds that are capable of interacting with a cysteine residue do *not* have roughly equal activity.

It is also noteworthy that the *ortho* morpholine group present in entries 1 and 7 enhances activity, since both the electron-donating effect of this group, as well as the steric hindrance it imparts, would *deactivate* the sulfur atom in the benzoisothiazolidone ring for nucleophilic attack. This again indicates that the morpholine ring present in the probe plays a positive role in IDE recognition that overrides its deleterious effects upon ligand reactivity.

3.5   Cellular Activity

The uHTS primary assay is cell-based, so all hits (and the probe) demonstrate cellular activity. As shown in **Figure 10** for the uHTS hit, cell-based EC_{50} is typically within 2- to 5-fold of biochemical IC_{50}.

3.6   Profiling Assays

In order to ascertain the *selectivity* of ML345 for IDE over other enzymes in the proteome with reactive cysteine residues, a proteome-wide activity-based protein profiling (ABPP) assay was conducted in collaboration with Ben Cravatt and Andrea Zuhl at TSRI-La Jolla. These assays were performed with the general cysteine-reactive probe chloroacetamide-rhodamine (CA-Rh)[33-35]. Briefly, the probe compound was incubated for 30 minutes at 37 °C in HEK293T proteomes then labeled for 30 minutes with 5 µM CA-Rh at 25 °C.   Analysis by SDS-PAGE and in-gel fluorescence scanning gave the results shown below in **Figure 14**.
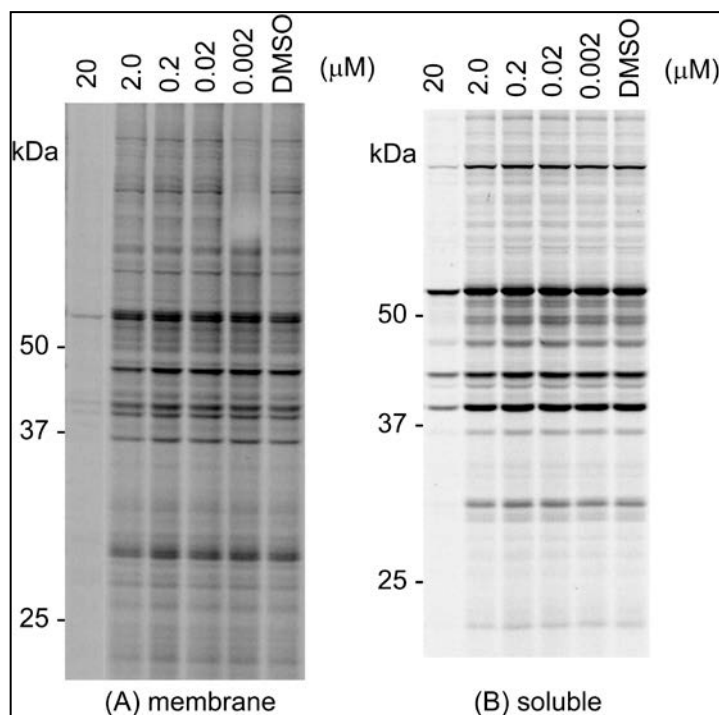

Figure 14. Proteome-wide activity-based protein profiling for cysteine reactivity of ML345

When ML345 was added to either membrane (A) or soluble (B) proteomes at concentrations of 2.0 µM or below, it did not inhibit labeling of cysteine-reactive proteins as determined by the retention of fluorescence signal compared to a DMSO control lane.   For both proteome fractions, ML345 was significantly reactive at 20 µM, as indicated by bands that do not appear in that lane using the highest concentration of test compound. Overall these results show that the probe is not a broadly reactive "cysteine trap" and that it likely has on the order of at least 10-fold selectivity for IDE in a whole cell environment.

Ideally the proteome-wide profiling assay would be complemented by profiling assays, especially including thio-reactive enzymes. Such assays much be thiol-free to have meaningful results, however, and a suitable thiol-free "ready to go" panel was not available from screening vendors. We hope to gather profiling data against related targets in the future, however.

4 Discussion

The identified probe ML345 will serve as a valuable tool for investigators interested in exploring the endogenous function of IDE, particularly aspects of its role in diabetes and Alzheimer's disease.

4.1 Comparison to existing art and how the new probe is an improvement

Prior art compounds that act as inhibitors of IDE are known, but none are both potent (IDE IC_{50} or EC_{50} <1 μM) and truly selective for IDE (**Figure 15**). These compounds include the cyclic peptide bacitracin (which has very low potency), chloroquine, 4-chloromercuribenzenesulfonate (aka PCMBS; CID11136; a highly cytotoxic compound)[36], and related p-chloromercuribenzoic acid (PCMBA). Weak and non-selective thiol-alkylating agents such as N-ethyl maleimide (NEM) and 2-iodoactetamide are known, as are weak and non-selective general zinc chelators such as 1,10-phenanthroline and EDTA[37]. IDE can also be inhibited in a dose-dependent manner with excess insulin[37,38]. Long-chain fatty acids and related acyl-CoA thioesters, such as linoleoyl-CoA and palmitoyl-CoA, act as IDE inhibitors with *in vitro* IC_{50} values ~10 µM and above[39]. ATP also inhibits IDE activity *in vitro*[37]. The protease inhibitor nelfinavir has been reported to inhibit insulin degradation mediated by partially purified IDE in cell-based assays; however, the IC_{50} was found to be greater than 100 µM[39].
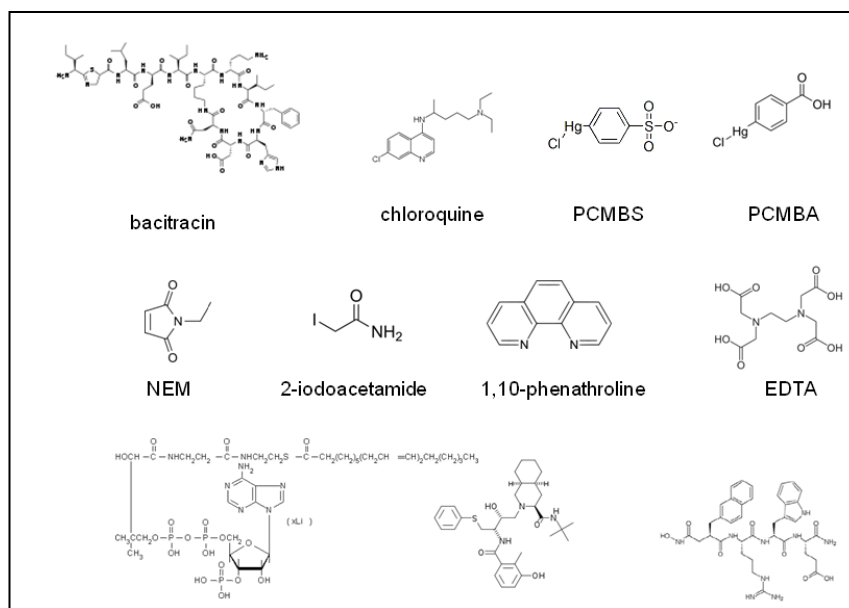

Figure 15. Prior art compounds. Exceptionally weak, non-selective, and non-drug-like prior art IDE inhibitors are *not* suitable starting points for small molecule probe development.

Recently, and subsequent to the initiation of this project, a peptide hydroxamic acid inhibitor of IDE that is highly potent (K_i for insulin ~23 nM) was developed by the assay submitter, Dr. Leissring[5]. However, this compound suffers from several limitations. First, due to its peptidic nature its utility *in vivo* is limited, which also limits its prospects for development into a more

drug-like probe. Second, it is not a small molecule, with a molecular weight ~750 Daltons. Finally, the hydroxamic acid group present in this IDE inhibitor is a promiscuous zinc-binding moiety which will likely cross-react with other zinc-metalloproteases, thereby limiting its specificity.

From the above analysis, the potent and selective small molecule IDE inhibitor ML345 is well-differentiated from existing art and will be a significant advance in the field.

4.2 Mechanism of Action Studies

We made significant efforts to show precisely how benzoisothiazolidones, including the probe ML345, interact with IDE. Much of this work was performed using the uHTS hit, CID 2325815. This compound and its analogs similarly studied display activity in the cell-based IDE inhibition assays (AIDs 434962, 435028, 463220, and 588712) and also consistently have higher activity in related cell-free biochemical assays (AIDs 688711 and 624067). Typically a two- to ten-fold cell-based shift is seen, typical of the barrier to cell penetration seen for most effective on-target small molecules.

We were interested in testing the proposed covalent mechanism of action of this series of compounds (see **Figure 9**, in section 3.1). Toward this end, mutant forms of IDE that have alanine replacements for either Cys-819 or Cys-812 were prepared[25] and used in IDE inhibition assays. The benzoisothiazolidone screening hit CID 2325815, an inhibitor of the native IDE enzyme with an IC_{50} = 1.4 μM (**Table 5**) *does not* inhibit mutant IDE lacking Cys-819 (IC_{50} >100 μM), though this compound is an inhibitor of the mutant enzyme lacking Cys-812 but with Cys-819 intact (IC_{50} ~3 μM). This shows that benzoisothiazolidones are *not* indiscriminately reactive, since they can distinguish between these two cysteine residues of IDE, preferentially reacting at Cys-819 to inhibit the enzyme.

The covalent mechanism of action for ML345 was further confirmed by using electrospray ionization-mass-spectrometry (ESI-MS) to show that ML345 bonds covalently to a thiol-containing cysteine analog present in large excesss (N-acetylcysteine), yielding a product of the predicted mass (625.2 amu).

Finally, the inhibition of IDE by ML345 was shown to be reversible by addition of reducing agents, such as ß-mercaptoethanol or dithiothreitol (data not shown).

These experiments, along with non-flat SAR (**Table 5** in Section 3.4), and combined with the results of the activity-based protein profiling experiment (**Figure 14** in section 3.6) show that *potent benzoisothiazolidones are direct, covalent, and reversible inhibitors of wild-type IDE that act preferentially at Cys-819 in the internal cavity of IDE.*

4.3 Planned Future Studies

Professors Leissring, Bannister, and collaborators intend to extend and expand upon this work through future grant proposals. Such efforts, if funded, will aim to develop a diverse set of potent, selective, IDE inhibitors, including zinc-targeting IDE inhibitors, more potent cysteine-targeting IDE inhibitors, and compounds in each class that are particularly suited for animal use, while also further studying mechanistic aspects of IDE inhibition by these compounds.

4.4 Acknowledgement

5 References

1.   Abdul-Hay SO, Kang D, McBride M, Li L, Zhao J, and Leissring MA. Deletion of insulin-degrading enzyme elicits antipodal, age-dependent effects on glucose and insulin tolerance. *PLoS ONE*, **2011**. 6(6), e20818. PMCID: PMC3111440

2.   Farris W, Mansourian S, Chang Y, Lindsley L, Eckman EA, Frosch MP, Eckman CB, Tanzi RE, Selkoe DJ, and Guenette S. Insulin-degrading enzyme regulates the levels of insulin, amyloid beta-protein, and the beta-amyloid precursor protein intracellular domain *in vivo*. *Proc Natl Acad Sci U S A*, **2003**. 100(7), 4162-7. PMCID: PMC153065

3.   Leissring MA, Farris W, Chang AY, Walsh DM, Wu X, Sun X, Frosch MP, and Selkoe DJ. Enhanced proteolysis of beta-amyloid in APP transgenic mice prevents plaque formation, secondary pathology, and premature death. *Neuron*, **2003**. 40(6), 1087-93. PMID: 14687544

4.   Li Q, Ali MA, and Cohen JI. Insulin degrading enzyme is a cellular receptor mediating varicella-zoster virus infection and cell-to-cell spread. *Cell,* **2006**. 127(2), 305-16. PMID: 17055432

5.   Leissring MA, Malito E, Hedouin S, Reinstatler L, Abdul-Hay SO, Choudhry S, Fauq AH, Huzarska M, May PS, Choi S, Logan TP, Turk BE, Cantley LC, Manolopoulou M, Tang WJ, Stein RL, Cuny GD, and Selkoe DJ. Designed inhibitors of insulin-degrading enzyme regulate the catabolism and activity of insulin. *PLoS One*, **2010**. 5(5), e10504. PMCID: PMC2866327

6.   Shearer JD, Coulter CF, Engeland WC, Roth RA, and Caldwell MD. Insulin is degraded extracellularly in wounds by insulin-degrading enzyme (EC 3.4.24.56). *Am J Physiol,* **1997**. 273(4 Pt 1), E657-64. PMID: 9357792

7.   Makarova KS and Grishin NV. Thermolysin and mitochondrial processing peptidase: how far structure-functional convergence goes. *Protein Sci,* **1999**. 8(11), 2537-40. PMID: 10595562

8.   Becker AB and Roth RA. Insulysin and pitrilysin: insulin-degrading enzymes of mammals and bacteria. *Methods Enzymol,* **1995**. 248, 693-703. PMID:7674956

9.   Mirsky IA and Broth-Kahn RH. The inactivation of insulin by tissue extracts. I. The distribution and properties of insulin inactivating extracts (insulinase*). Arch Biochem*, **1949**. 20, 1-9. PMID:18104389

10.   Mirsky IA and Perisutti G. Effect of insulinase-inhibitor on hypoglycemic action of insulin. *Science*, **1955**. 122(3169), 559-60. PMID:13255892

11.   Mirsky IA, Perisutti G, and Diengott D. The inhibition of insulinase by hypoglycemic sulfonamides. *Metabolism*, **1956.** 5(2), 156-61. PMID:13296877

12.   Mirsky IA, Perisutti G, and Gitelson S. The role of insulinase in the hypoglycemic response to sulfonylureas. *Ann N Y Acad Sci*, **1957**. 71(1), 103-11. PMID:13459205

13.   Marigo S and Panelli G. Insulinase and its inhibition by hypoglycemic sulfonamides; data on insulin sensitivity during tolbutamide therapy. *Arch Sci Med (Torino),* **1958**. 105(6), 587-609. PMID:13560210

14.   Leites SM and Smirnov NP. Significance of insulin-inactivating properties of the liver (insulinase) in the mechanism of action of antidiabetic sulfonamides. *Bull Eksp Biol Med*, **1959**. 47(6), 58-62. PMID:13671070

15.   Leissring MA and Selkoe DJ. Structural biology: enzyme target to latch on to. *Nature*, **2006**. 443(7113), 761-2. PMID:17051198

16.   Shen Y, Joachimiak A, Rosner MR, and Tang W-J. Structures of human insulin-degrading enzyme reveal a new substrate mechanism. *Nature*, **2006**. 443(7113), 870-4. PMCID: PMC3366509

17.   Cabrol C, Huzarska MA, Dinolfo C, Rodriguez MC, Reinstatler L, Ni J, Yeh L-A, Cuny GD, Stein RL, Selkoe DJ, and Leissring MA. Small-molecule activators of insulin-degrading enzyme discovered through high-throughput compound screening. *PLoS ONE,* **2009**. 4(4), e5274. PMCID: PMC2668070

18.   Leissring MA, Farris W, Turk BE, Cantley LC, Yeh L, Caclin C, Xing X, Cuny GD, Stein RL, and Selkoe DJ. Small-molecule inhibitors of insulin-degrading enzyme. *Society for Neuroscience Abstract Viewer/Itinerary Planner*, **2004**. Program No. 488.11(online).

19.   Leissring MA, Logan TP, Choi S, Cuny GD, Turk B, Cantley LC, Farris W, and Selkoe DJ. Rationally designed peptide hydroxamate inhibitors of insulin-degrading enzyme. *Society for Neuroscience Abstract Viewer/Itinerary Planner*, **2005.** Program No. 134.11(Online).

20.   Yonezawa K, Yokono K, Shii K, Hari J, Yaso S, Amano K, Sakamoto T, Kawase Y, Akiyama H, Nagata M, and et al. Insulin-degrading enzyme is capable of degrading receptor-bound insulin. *Biochem Biophys Res Commun*, **1988**. 150(2), 605-14. PMID:3277630

21.   Seta KA and Roth RA. Overexpression of insulin degrading enzyme: cellular localization and effects on insulin signaling. *Biochem Biophys Res Commun*, **1997**. 231(1), 167-71. PMID:9070242

22.   Leissring MA. The AßCs of Aß-cleaving proteases. *J Biol Chem*, **2008**. 283(44), 29645-9. PMCID: PMC18723506

23.   Turner AJ and Nalivaeva NN. New insights into the roles of metalloproteinases in neurodegeneration and neuroprotection. *Int Rev Neurobiol*, **2007**. 82, 113-35. PMID:17678958

24.   Manolopoulou M, Guo Q, Malito E, Schilling AB, and Tang WJ. Molecular basis of catalytic chamber-assisted unfolding and cleavage of human insulin by human insulin degrading enzyme. *J Biol Chem*, **2009**. 284(21), 14177-88. PMID:19321446

25.   Neant-Fery M, Garcia-Ordonez RD, Logan TP, Selkoe DJ, Li L, Reinstatler L, and Leissring MA. Molecular basis for the thiol sensitivity of insulin-degrading enzyme. *Proc Natl Acad Sci U S A*, **2008**. 105(28), 9582-7. PMCID: PMC2474492

26. Brothers SP, Saldanha SA, Spicer TP, Cameron M, Mercer BA, Chase P, McDonald P, Wahlestedt C, and Hodder PS, Selective and brain penetrant neuropeptide Y Y2 receptor antagonists discovered by whole-cell high-throughput screening. *Mol Pharmacol*, **2010**. 77(1), 46-57. PMID: 2802430.

27. Singh J, Petter RC, Baillie TA, Whitty A. The resurgence of covalent drugs. *Nature Reviews Drug Discovery,* **2011**. 10, 307-317. PMID: 21455239

28. Lipinski CA, Lombardo F, Dominy BW, and Feeney PJ, Experimental and computational approaches to estimate solubility and permeability in drug discovery and development settings. *Advanced Drug Delivery Reviews*, **2001**. 46, 3–26. PMID:11259830

29. Walters WP, Going further than Lipinski's rule in drug design. *Expert Opinion on Drug Discovery*, **2012**. 7(2), 99-107. PMID:22468912

30. Rishton GM, Nonleadlikeness and leadlikeness in biochemical screening. *Drug Discovery Today*, **2003**, 8(2), 86-96. PMID:12565011

31. Benigni R and Bossa C, Mechanisms of Chemical Carcinogenicity and Mutagenicity: A Review with Implications for Predictive Toxicology. *Chem Rev*, **2011**. 111(4), 2507-2536. PMID:21265518

32. Dahl R, Bravo Y, Sharma V, Ichikawa M, Dhanya R-P, Hedrick M, Brown B, Rascon J, Vicchiarelli M, Mangravita-Novo A, Yang L, Stonich D, Su Y, Smith LH, Sergienko E, Freeze HH, and Cosford NDP, Potent, Selective, and Orally Available Benzoisothiazolone Phosphomannose Isomerase Inhibitors as Probes for Congenital Disorder of Glycosylation Ia. *J. Med. Chem.* **2011**. 54, 3661–3668. PMID:21539312

33. Weerapana E, Simon GM, and B.F. Cravatt BF. Disparate proteome reactivity profiles of carbon electrophiles. *Nature Chemical Biology*, **2008**. 4(7), 405-407. PMID: 18488014

34. Bachovchin DA, Zuhl AM, Speers AE, Wolfe MR, Weerapana E, Brown SJ, Rosen H, Cravatt BF. Discovery and Optimization of Sulfonyl Acrylonitriles as Selective, Covalent Inhibitors of Protein Phosphatase Methylesterase-1. *Journal of Medicinal Chemistry,* **2011**. 54(14), 5229-5236. PMID: 21639134

35. Weerapana E, Wang C, Simon GM, Richter F, Khare S, Dillon MB, Bachovchin DA, Mowen K, Baker D, Cravatt BF, Quantitative reactivity profiling predicts functional cysteines in proteomes. *Nature.* **2010**. 468, 790-795. PMID:21085121

36. Duckworth, WC, Hamel, FG and Peavy, DE, Two pathways for insulin metabolism in adipocytes. *Biochim Biophys Acta*, **1997**. 1358(2), 163-71. PMID:9332452

37. Del Carmen Camberos M and Cresto JC, Insulin-degrading enzyme hydrolyzes ATP. *Exp Biol Med (Maywood),* **2007**. 232(2), 281-92. PMID:17259336

38. Farris, W, Mansourian, S, Chang, Y, Lindsley, L, Eckman, EA, Frosch, MP, Eckman, CB, Tanzi, RE, Selkoe, DJ and Guenette, S, Insulin-degrading enzyme regulates the levels of insulin, amyloid beta-protein, and the beta-amyloid precursor protein intracellular domain *in vivo*. *Proc Natl Acad Sci U S A*, **2003**. 100(7), 4162-7. PMID:12634421

39. Hamel FG, Upward JL and Bennett RG, *In vitro* inhibition of insulin-degrading enzyme by long-chain fatty acids and their coenzyme A thioesters. *Endocrinology*, **2003**. 144(6), 2404-8. PMID:12746301